Spectral imaging

Kehinde Oyemakinwa, Shafiul Alam, Aleksi Leinonen

Laboratory Practice Report
December 2017
Department of Physics and Mathematics
University of Eastern Finland

K. Oyemakinwa, S. Alam, A. Leinonen *Spectral imaging*, 19 pages
University of Eastern Finland
Master's Degree Programme in Photonics

Supervisors Ph.D. Hannu Laamanen

Abstract

In this work the concept of spectral imaging was studied and samples were measured using LCTF for five various lens system. From these samples reflectance and radiance was obtained. Reflectance and radiance curves were plotted and used to determine which objective gives the best reflectance and radiance. Tokina-Macro 100 mm was found to be the best objective but other objectives could be equally good if all errors are accounted for and can be reduced considerably.

Contents

Chapter I

Introduction

Human has certain limitation in processing spectral data that is due to the functional limitation of our eyes. The reason is that our retina has trichromatic nature which means human retina captures light by three types of color sensors and as a result we can observe only a part of spectral information. However some animals have more color sensors and therefore they can observe more colors than human. So the main limitation of human eye of capturing spectral information is due to the number and wavelength range of color sensors and this limitation can be avoided by introducing a technology with higher wavelength resolution and wider wavelength range. Spectral imaging is such a technique through which we can achieve such artificial hypervision. [1]

Spectral imaging is a relatively new technology which is a combination of conventional imaging and spectroscopy that provides information about the spatial and spectral information of a sample. Spectral imaging also known as imaging spectroscopy was first introduced by Goetz in 1980. Depending on the spectral resolution and properties of bands, spectral imaging can be divided into three different categories: multispectral imaging, hyperspectral imaging (HSI) and ultraspectral imaging. The main difference between multispectral and hyperspectral imagery is in spectral resolution. While multispectral imaging contains data from 3-10 wider bands, the hyperspectral imaging collects data from hundreds of spectral bands. Ultraspectral imaging collects information from even more spectral bands. [2]

Spectral imaging can be used for medical purposes especially for diagnosis and surgery as it gives the physiology, morphology as well as the composition of the sample. Apart from these it is also used in Archeology and Museum, Food industry, Remote Sensing and in Forensic sector. [3]

In this study, a Liquid Crystal Tunable Filter camera (LCTF) was used, which can perform spectral imaging over a wide range of wavelengths. The purpose of this study is to find out how the angle of incident light and the focal length of the objective affects the measuring results of the LCTF. For this reason, five different objectives were used for measuring the spectral radiance and reflectance of a color checker chart.

In the second chapter theoretical aspect of spectral imaging is introduced. Here, the mechanism of LCTF as well as the spectral cube will be discussed. Also, theoretical background of reflectance calculations, effect of focal length, f-number and field of view will also be explained. The third chapter discusses the measurement procedure and calculation of reflectance and radiance. In this chapter results of the work will also be discussed. Conclusions will be given in the last chapter.

Chapter II

Theory

There are several basic concepts that sum up in achieving the desired results when carrying out research in the field of spectral imaging. In this chapter, a brief description of basic concepts employed in the capturing of data from samples and evaluation of the data captured are discussed.

2.1 Spectral cube

A spectral image is a combination of imaging and spectroscopic techniques. An imaging system provides two dimensional information of the intensity of the pixels on (x, y) plane while spectroscopy gives one dimensional information about the wavelength λ. When both of these techniques are integrated together in spectral imaging, the result generated is a 3D data set that can be termed a spectral data cube, as presented in fig. 2.1. [4]

Hence, a spectral data cube contains both spatial information and spectral information simultaneously. This spectral cube provides a luxury of information which can be manipulated or used for analysis. The pixels captured by the detector provide the spatial information which are representative of the (x, y) plane while the spectral information is given by the corresponding wavelengths λ equivalent to the z-plane. The cube therefore gives information of the pixels within the range of wavelengths used. [4]

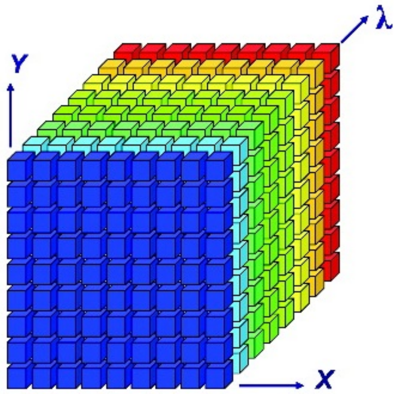

Figure 2.1: Spectral cube. [4]

2.2 Reflectance calculations

When light is incident upon a surface, the surface responds in three ways: light is either transmitted, absorbed by the surface or reflected by the surface. The amount of reflected light normalized by the incident light is called the reflectance R

$$R = I/I_0, \tag{2.1}$$

where I is the reflected intensity and I_0 is the intensity incident on the surface in question. [5]

Spectral reflectance is a vital parameter in evaluating how the various points on the surface of the material respond when exposed to light. The spectral reflectance measured is a measure of the reflected light to the incident light on the surface as a function of wavelength. As the wavelength changes, the reflectance of a surface also varies because light is either scattered or absorbed at certain wavelengths [5]. This report takes into account the spectral data cubes generated from the measurements of the color checker rendition chart and a white reference sample. The spectral reflectance was then calculated by dividing the spectral data cube of the color checker by the spectral data cube of the white reference.

2.3 LCTF camera

In this study, a liquid crystal tunable filter (LCTF) camera was used to measure samples. LCTF camera is a filter based spectral imaging system with a wavelength range usually varying from VIS to NIR [6]. LCTF cameras offer high acceptance angles, almost no moving mechanical parts, are compact and flexibile thus making them attractive choice for spectral imaging [6, 7]. In this laboratory practise a Nuance EX LCTF camera was used. It has a spectral range from 450 nm to 950 nm.

LCTF consists of multiple stages that are stacked and the sum of these stages provides us the desired spectral range. One stage consists of two parallel linear polarizers, a retarder made of birefringent material, and a liquid crystal layer that is electronically controlled and placed in between the polarizers. This combination functions as a bandpass filter that can be adjusted electronically. A schematic drawing of one stage is provided in Fig. 2.2. [6, 7]

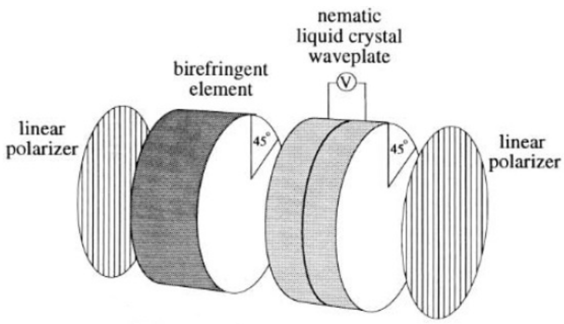

Figure 2.2: One stage of LCTF. [7]

When light enters the LCTF stage, it is separated into two rays: ordinary and extraordinary rays. These rays have different optical path lengths inside the birefringent retarder, which causes these rays to have a phase difference. This phase difference is dependent on the wavelength of the light. The polarizer located after the retarder transmits only the light in phase through to the next stage and thus act as the input polarizer for the next stage. Every stage of the LCTF transmits the light as a sinusoidal function of the wavelength. The frequency of this function is defined by the thickness of the retarder and the difference between the refractive indices of ordinary and extraordinary rays. [6, 7]

The combination of these invidual filter stages produce a narrow spectral band. This band can be modified by adjusting the electric potential of the liquid crystal cell. In total this system allows the measurement of a large spectral band due to the electrical tunability of the liquid crystal cell. Although the spectral band can be wide, it is limited by the components and can thus accommodate only a specific spectral band. [6, 7]

Transmittance for different spectral bands in Nuance EX is not equal. This difference is compensated in the software by normalizing the gained intensity on the detector with a longer exposure time. If one would prefer to measure radiance or intensity using LCTF they should take the effect of exposure time into account. For Nuance EX the exposure time data can be directly obtained from the software.

2.4 Effect of focal length, f-number and field of view

The focal length f of the system defines the point at which the image will focus on. It also defines the field of view of an optical system. The further away we focus the image, the smaller the field of view gets. Thus smaller focal length f will give a larger field of view. [5]

The amount of collected light given by an optical system is the f-number of the system. f-number $f/\#$ is defined as

$$f/\# = \frac{f}{D}, \tag{2.2}$$

where f is the focal length and D is the diameter of the entrance pupil of the optical system. As can be seen from Eq. (2.2) the f-number actually decreases when the amount of collected light increases. This is due to the inverse dependency on the lens diameter D. One interesting charasteristic of f-number $f/\#$ is the way it is referred to. f-number $f/\#$ is understood as a single symbol, where $\#$ is the f-number of the system. For example a system with f-number of 2 is written as $f/2$. [5]

Chapter III

Measurements and calculations

This chapter discusses the measurement set-up, step by step analysis of how calculations were done and some observations discovered in the results obtained.

3.1 Measurement Procedure

The light source used is a Gretag MacBeth Spectralight III light booth, which can generate simulated D65 daylight, which was used in measurement. In the beginning of measurement the light source was stabilized for two hours. The Nuance EX LCTF camera was mounted on a tripod. Five different objective lens systems were used with different focal length namely: Nikon-Macro 60 mm, Sigma-Macro 28 mm, Nikon-Macro 20 mm, Nikon-Macro 16 mm, Tokina-Macro 100 mm. The exposure time for the white reference was recorded. LCTF filters have different transmittance and thus are compensated by exposure time. After measuring the exposure time, the spectral cube for white reference and color checker was captured. During measurement the objective and samples were placed perpendicularly to each other. The distance between samples and camera were different for different focal lengths and the distance was set so the field of view will cover the sample horizontally. The f-number was chosen as $f/4$ for all objectives. The experiment was done in a dark room so the samples were not exposed to other light sources apart from the light booth.

3.2 Reflectance

As in the structure of the measurement procedure discussed above, light incident on the reference white sample and the color checker sample has been used to obtain a reflectance spectrum across every point on the surface of the samples. As stated in chapter two, the reflectance measurements for the color checker has been divided by the reflectance of the white reference to get the reflectance R of the spectrum as shown in Eq.(3.1)

$$R(\lambda) = \frac{S_{\text{sample}}(\lambda)}{S_{\text{white}}(\lambda)}. \tag{3.1}$$

In discussing the results obtained, different sample points were chosen particularly at the edges of the color checker to investigate the effect of focal length and transmittance of light on the reflectance of the color checker. It is important to note here that the same color checker and white reference sample has been used for the objectives with different focal length. Also the reflectance has been plotted for the same sample points on the color checker for the objectives. Seven sample points were taken as shown in Fig. 3.1 and the reflectance plots generated for each sample points are shown in Figs. A.1 - A.4.

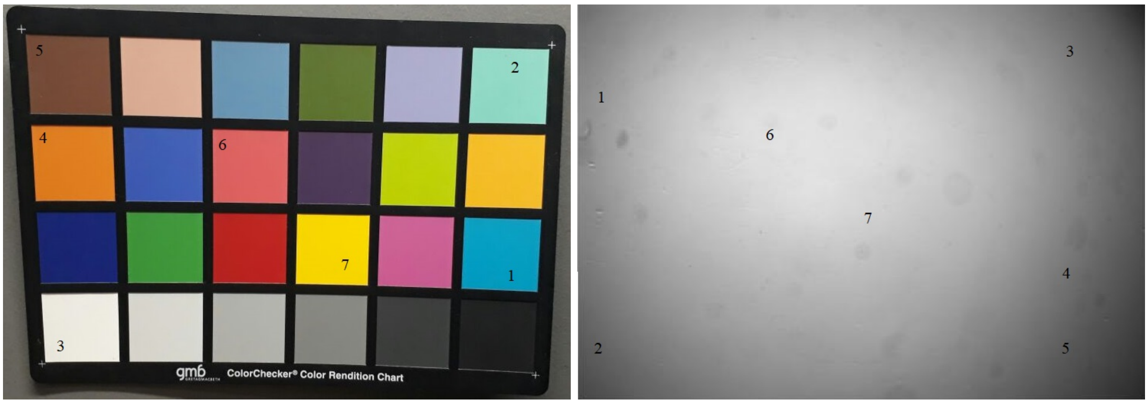

(a) Sample points on color checker. (b) Sample points on white reference.

Figure 3.1: Used sample points for calculations.

As observed, the reflectance curves for all five objectives at the various points chosen have the same pattern with only small variations in magnitude. It can also be seen from Fig. 3.1 that the image of the color checker is inverted due to how measurements were taken.

Nikon-macro 60 mm and Sigma-Macro 28 mm were observed to have higher reflectance ratio curves than the other lenses. This disparity could have been caused if the color checker was placed at different locations when these measurements were carried out. Also, the white reference was not clean and as a result the reflectance values calculated were affected. It could also be that the objectives were dirty coupled with the fact that the position of the white reference sample was not placed in the same orientation as for the other objectives thereby changing the reflectance values generated during calculation.

The measurements for Nikon-Macro 60 mm and Sigma-Macro 28 mm were taken on the same day while the other objectives were taken on another day. The measurements were repeated for Tokina-Macro 100 mm and Sigma-Macro 28 mm which were taken at different times. Calculations based on this new data were done to obtain the reflectance plot shown in Fig. 3.2. The two objectives showed the same pattern for their reflectance curves which are different from the other objectives. This suggests possible errors in the first measurements done for the objectives and therefore it is imporant to ensure the measurements are carried out on the same day under the same condition. Further observatios will be discussed in the radiance calculation.

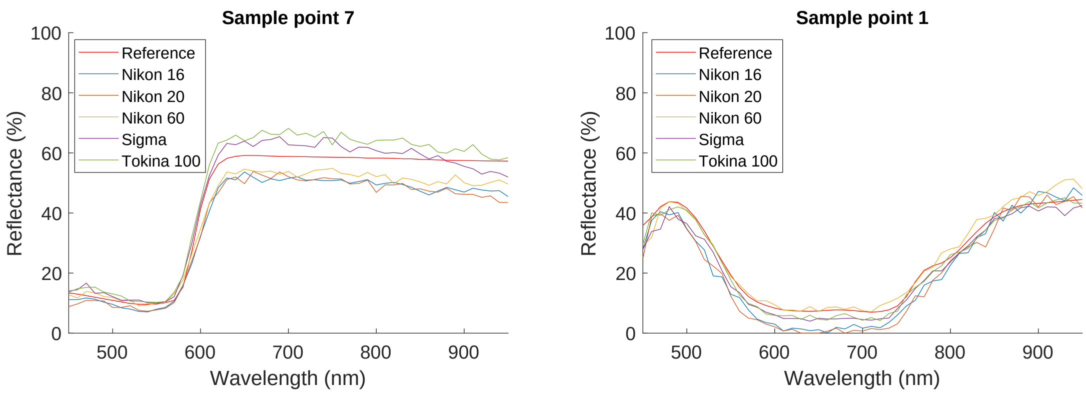

(a) Reflectance for sample point 7.

(b) Reflectance for sample point 1.

Figure 3.2: Two reflectance curves plotted from spectral data. Sigma and Tokina lenses are from the second measurement used to correct data.

Now, the difference observed in the first measurements is considerably reduced ($\approx$ 10%), which confirms the disparity seen earlier. This can be seen in Fig. 3.3. The observation of some spots on white reference as shown in Fig. 3.1b and Fig. 3.4

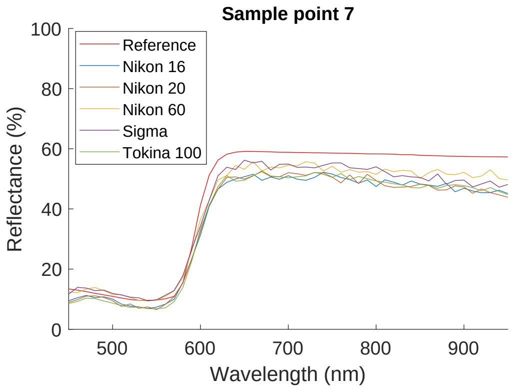

(a) Reflectance for old measurements on sample point 7.

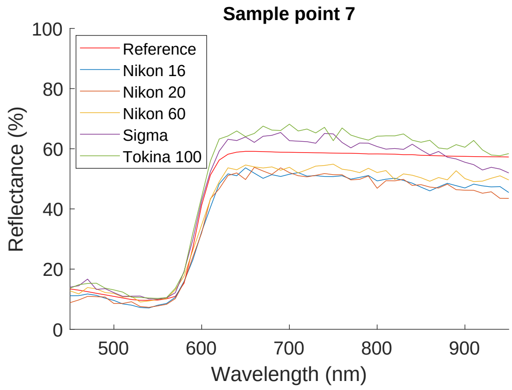

(b) Reflectance for new measurements for Sigma and Tokina on sample point 7.

Figure 3.3: Two reflectance curves plotted from spectral data.

could be the major reason for the errors observed in the reflectance calculation and subsequently in the reflectance plot. Care should be taken to ensure the samples used are kept clean and free of surface contact.

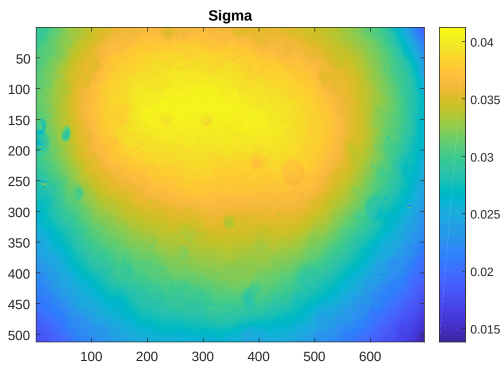

Figure 3.4: Pseudocolored image of white reference.

3.3 Radiance

The observations so far reveal that the focal length f of the objectives have no significant effect on the reflectance of the objectives. However, the question of which objective gives the best result and should be used for laboratory practices still arises. The reflectance calculation, as mentioned earlier, having the same pattern for all objectives is not sufficient to answer this question. In order to answer the question, the radiance of the LCTF camera for all objectives was taken into consideration.

To do this, measurements of the radiance of the white reference sample was taken using Konica Minolta CS 2000 Spectroradiometer. This gives the actual data for the radiance of the white reference at the center point of the reference denoted $M(\lambda)$. Then the normalized measured power of light from the LCTF camera at one pixel was calculated denoted by $S_C(\lambda)$. $S_C(\lambda)$ was calculated by dividing the measured power $S(\lambda)$ with the relative exposure time $T_r(\lambda)$, as:

$$S_C(\lambda) = S(\lambda)/T_r(\lambda). \tag{3.2}$$

The relative exposure time $T_r(\lambda)$ was calculated by taking the ratio of the exposure time of a wavelength $T(\lambda)$ and the minimum exposure time recorded $T_{\min}$:

$$T_r(\lambda) = T(\lambda)/T_{\min}. \tag{3.3}$$

This accounts for the compensation in the transmittance of the LCTF discussed in section 2.3.

Corrections for the radiance were calculated by taking the ratio of radiometric measurements $M(\lambda)$ and the normalized power of light $S_C(\lambda)$ which is the correlation coefficient $C(\lambda)$:

$$C(\lambda) = M(\lambda)/S_c(\lambda). \tag{3.4}$$

The correlation coefficient $C(\lambda)$ varies between objectives and the transmittance of LCTF cells used. This is due to changing exposure times as discussed in section 2.3 and it can be seen from Eqs. (3.2) and (3.3). The change in correlation coefficient between objectives and wavelengths can be seen in Fig. 3.5.

Radiance was calculated for an average of 10x10 pixels across all wavelengths. As a result radiance was plotted for all seven sample points shown in Fig. B.1 - B.4. The same sample points were used earlier to study reflectance. Fig. 3.6 shows how

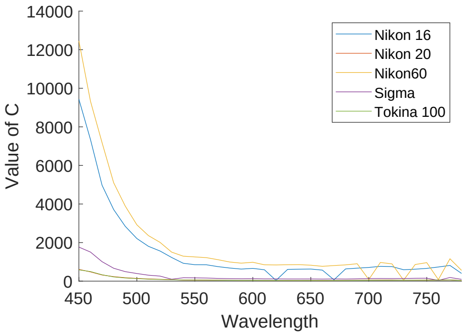

(a) Correlation coefficient curve $C(\lambda)$.

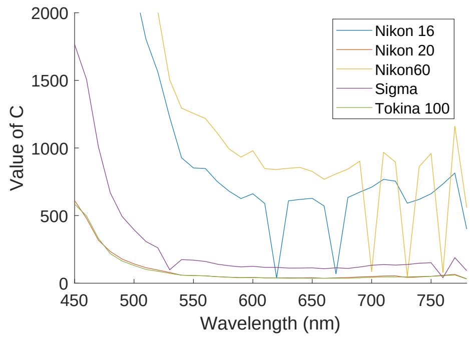

(b) Magnified correlation coefficient curve $C(\lambda)$.

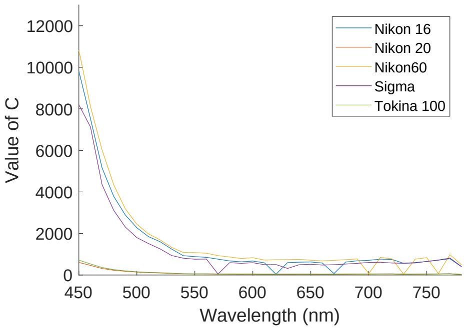

(c) Correlation coefficient curve $C(\lambda)$ for old data.

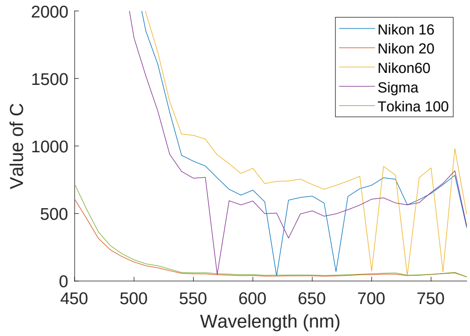

(d) Magnified correlation coefficient curve $C(\lambda)$ for old data.

Figure 3.5: The wavelength dependent normalization coefficient $C(\lambda)$ for all five objectives.

the radiance varies between the objectives with different focal lengths for sample points one and seven.

The correlation coefficient curve and its magnified view are shown in Fig. 3.5a and Fig. 3.5b for the first measurements and Fig. 3.6a and Fig. 3.6 for the new measurements respectively. As expected the radiance curve drops rapidly at the edges. However, the value of the correlation coefficient of Sigma-Macro 28 mm dropped from about 8000 to 1800 which is very huge. Tokina-Macro 100 mm and Sigma-macro 28 mm were also noticeed to have a closely related pattern for the correlation coefficient which confirms that errors may have been made in the first measurements as suggested earlier.

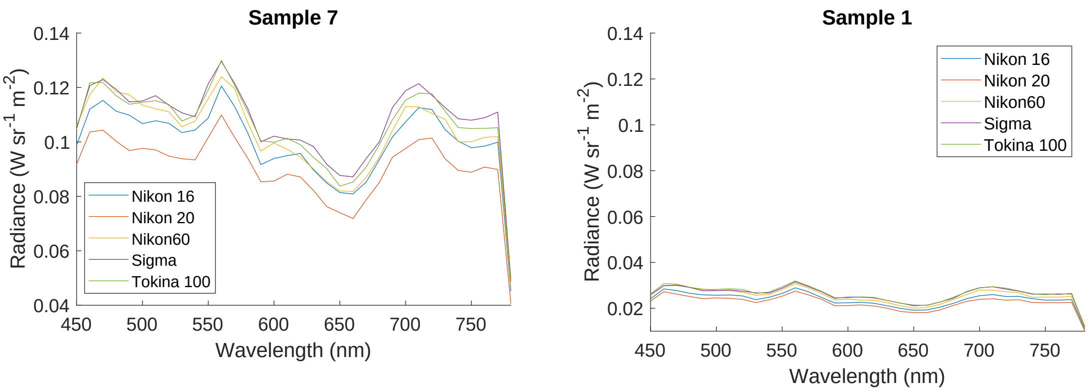

(a) Radiance for sample point 7. (b) Radiance for sample point 1.

Figure 3.6: Two reflectance curves plotted from spectral data. Sigma and Tokina lenses are from the second measurement used to correct data.

3.4 Choosing the best lens

In order to determine the best objective, the reflectances, radiances and correlation coefficients of lens systems were taken into account. Among all reflectance plots, Tokina-Macro 100 mm has the highest value especially when viewed from Fig. A.1b which shows the best reflectance pattern. Also, Tokina-Macro 100 mm gives the highest value for radiance plot coupled with the fact that it has the lowest correlation coefficient. Sigma-Macro 28 mm also gives similar patterns for all plots and considerable correlation coefficient but the reflectance plots do not match those of Tokina-Macro 100 mm. The other three objectives do not show similar pattern as Tokina-Macro 100 mm or Sigma-Macro 28 mm and thus are excluded. Overall it can be said that of all the objectives, Tokina-Macro 100 mm gives the best result.

Chapter IV
Conclusions

The color checker and white reference were used for measuring reflectance and the measurement was done by LCTF camera. For radiance measurement Konica Minolta CS 2000 spectrometer was used for white reference within 380 - 780 nm with 1 nm interval. A uniform light source was used with a spectral distribution of D65 daylight. Spectral cube within 450 - 950 nm wavelength with 10nm interval was obtained. Reflectance and radiance curves for 7 sample points was plotted for 450 - 950 nm and 380 - 780 nm wavelength region respectively. To compare the reflectance and radiance curves five objective lenses were used.

By comparing the reflectance and radiance curves it was found that Tokina-Macro 100 mm gave the best result. The measurement was done in three different days so the error in measurement may be due to the change in orientation of color checker and white reference. Apart from this, there was a possibility that the samples and objective lenses were dirty and the position of the LCTF may not be perfect. Also, the white reference was dirty which affected the results. In addition, the focusing of lenses may not be perfect.

When taking all the errors into account, it is possible that the differences between the lenses will disappear and thus all of the lenses may be equally good. This can only be confirmed in a further study.

Bibliography

[1] S. Nakauchi, *Spectral Imaging Technique for Visualizing the Invisible Information* (Springer Berlin Heidelberg, Berlin, Heidelberg, 2005), pp. 55–64.

[2] Q. Li, X. He, Y. Wang, H. Liu, D. Xu, and F. Guo, "Review of spectral imaging technology in biomedical engineering: achievements and challenges," *Journal of Biomedical Optics* **18**, 18 – 18 – 29 (2013).

[3] B. F. Guolan Lu, "Medical hyperspectral imaging: a review," *Journal of Biomedical Optics* **19**, 19 – 19 – 24 (2014).

[4] Y. Garini, I. T. Young, and G. McNamara, "Spectral imaging: Principles and applications," *Cytometry Part A* **69A**, 735–747 (2006).

[5] E. Hecht, *Optics*, 5th ed. (Addison Weasley, San Francisco, 2017).

[6] J. Qin, "5 - Hyperspectral Imaging Instruments," in *Hyperspectral Imaging for Food Quality Analysis and Control*, D.-W. Sun, ed. (Academic Press, San Diego, 2010), pp. 129 - 172.

[7] H. R. Morris, C. C. Hoyt, and P. J. Treado, "Imaging Spectrometers for Fluorescence and Raman Microscopy: Acousto-Optic and Liquid Crystal Tunable Filters," *Applied Spectroscopy* **48**, 857–866 (1994).

Appendix A
Reflectance figures

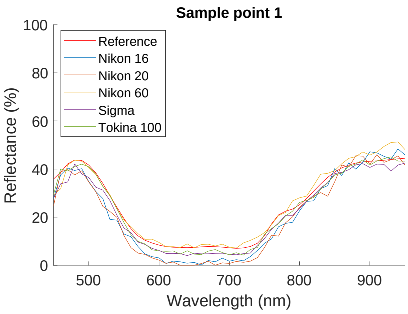

(a) Reflectance for sample point 1.

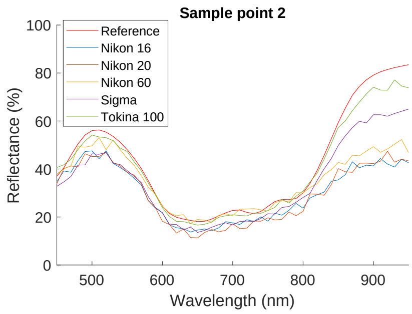

(b) Reflectance for sample point 2.

Figure A.1: Reflectance curves for sample points 1 and 2.

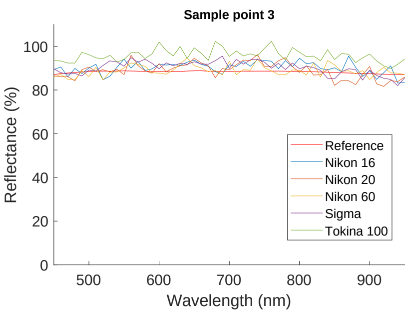

(a) Reflectance for sample point 3.

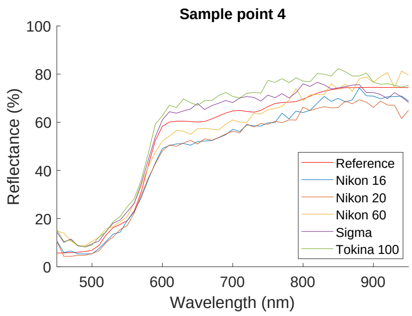

(b) Reflectance for sample point 4.

Figure A.2: Reflectance curves for sample points 3 and 4.

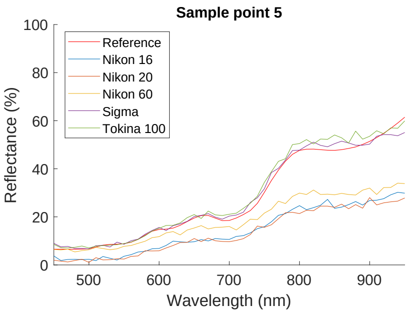

(a) Reflectance for sample point 5.

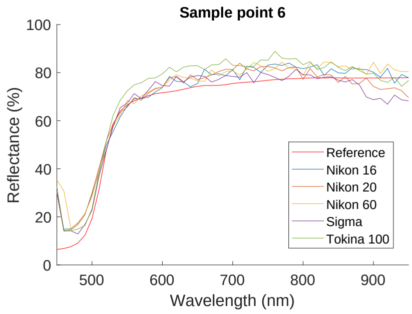

(b) Reflectance for sample point 6.

Figure A.3: Reflectance curves for sample points 5 and 6.

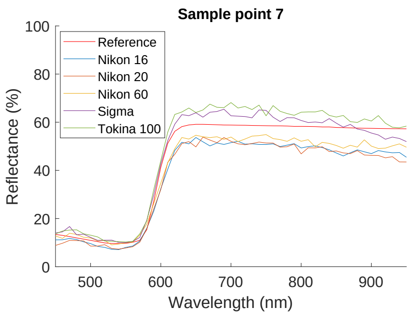

Figure A.4: Reflectance for sample point 7.

Appendix B
Radiance figures

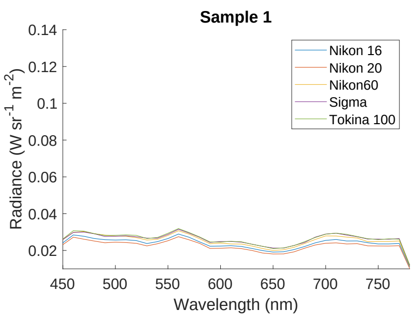

(a) Radiance for sample point 1.

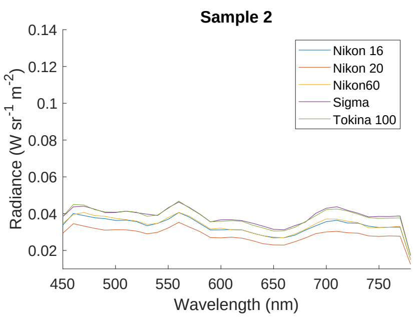

(b) Radiance for sample point 2.

Figure B.1: Radiance curves for sample points 1 and 2.

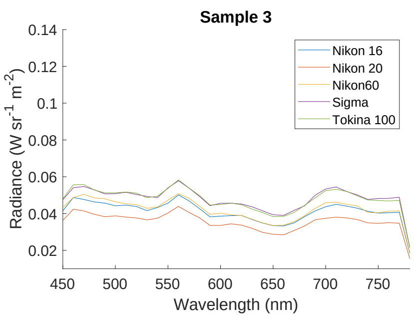

(a) Radiance for sample point 3.

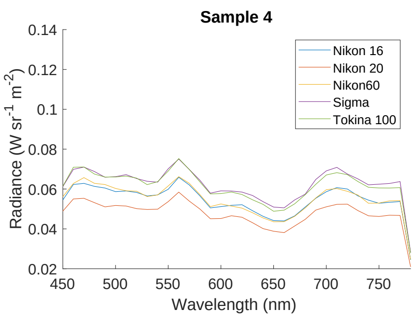

(b) Radiance for sample point 4.

Figure B.2: Radiance curves for sample points 3 and 4.

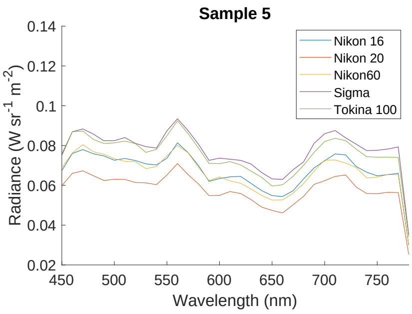

(a) Radiance for sample point 5.

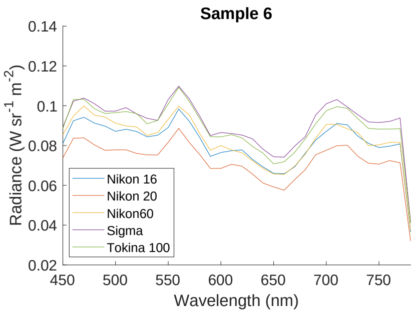

(b) Radiance for sample point 6.

Figure B.3: Radiance curves for sample points 5 and 6.

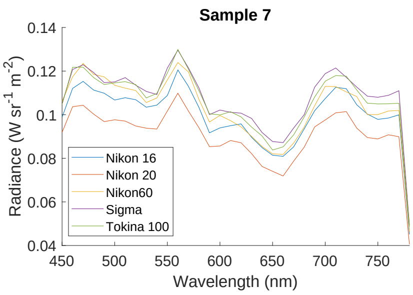

Figure B.4: Radiance for sample point 7.